

RML58F25

CONFIDENTIAL

Copy 196  
RM L58F25

UNCLASSIFIED



## RESEARCH MEMORANDUM

MEASUREMENTS OF THE BUFFETING LOADS ON THE WING  
AND HORIZONTAL TAIL OF A 1/4-SCALE MODEL  
OF THE X-1E AIRPLANE

By A. Gerald Rainey and William B. Igoe

Langley Aeronautical Laboratory  
Langley Field, Va.

CANCELLED

Classification

CHANGED TO *Unc.*By authority of *NASA T.P. #39 (2-16-61)*  
Changed by *ARL* Date *FEB 22 1967*

CLASSIFIED DOCUMENT

This material contains information affecting the National Defense of the United States within the meaning of the espionage laws, Title 18, U.S.C., Secs. 793 and 794, the transmission or revelation of which in any manner to an unauthorized person is prohibited by law.

NATIONAL ADVISORY COMMITTEE  
FOR AERONAUTICS

WASHINGTON

September 17, 1958

UNCLASSIFIED

CONFIDENTIAL



## NATIONAL ADVISORY COMMITTEE FOR AERONAUTICS

## RESEARCH MEMORANDUM

## MEASUREMENTS OF THE BUFFETING LOADS ON THE WING

AND HORIZONTAL TAIL OF A 1/4-SCALE MODEL

OF THE X-1E AIRPLANE\*

By A. Gerald Rainey and William B. Igoe

## SUMMARY

The buffeting loads acting on the wing and horizontal tail of a 1/4-scale model of the X-1E airplane have been measured in the Langley 16-foot transonic tunnel in the Mach number range from 0.40 to 0.90. When the buffeting loads were reduced to a nondimensional aerodynamic coefficient of buffeting intensity, it was found that the maximum buffeting intensity of the horizontal tail was about twice as large as that of the wing. Comparison of power spectra of buffeting loads acting on the horizontal tail of the airplane and of the model indicated that the model horizontal tail, which was of conventional force-test-model design, responded in an entirely different mode than did the airplane. This result implied that if quantitative extrapolation of model data to flight conditions were desired a dynamically scaled model of the rearward portion of the fuselage and empennage would be required.

A study of the sources of horizontal-tail buffeting of the model indicated that the wing wake contributed a large part of the total buffeting load. At one condition it was found that removal of the wing wake would reduce the buffeting loads on the horizontal tail to about one-third of the original value.

## INTRODUCTION

The need for a rational approach to the problem of designing efficiently for buffeting loads has long been recognized. The suggestive papers of Liepmann (refs. 1 to 3) have led to a series of investigations both in flight (refs. 4 and 5) and in wind tunnels (refs. 6 to 9). The results obtained indicate that a relatively straightforward wind-tunnel

---

\*Title, Unclassified.

technique is feasible for the prediction of the buffeting loads on an airplane wing if the model and the wind tunnel meet certain requirements. These requirements, which do not appear to be very severe, are discussed in some detail in reference 8.

It is of interest, however, to examine the applicability of this wind-tunnel technique to the problem of designing for the buffeting loads acting on the horizontal tail. In general, measurements of the buffeting loads experienced by airplanes have indicated that buffeting of the horizontal tail represents a more serious loads problem than does buffeting of the wing because the fluctuating loads acting on the horizontal tail are usually a larger percentage of the design load than are those acting on the wing.

Consequently, buffeting measurements have been made on the wing and horizontal tail of a 1/4-scale model of the X-1E research airplane in the Langley 16-foot transonic tunnel. The buffeting measurements were made in conjunction with a study of the wing and aileron flutter characteristics. The results of the flutter investigation have been reported in reference 10. The model used in the investigation had a wing that was dynamically scaled to simulate the airplane flutter parameters. The fuselage and empennage, however, were designed for static aerodynamic wind-tunnel tests.

Some of the results of this buffeting study, regarding the degree of applicability of this type of model design to tail buffeting investigations, have already been presented in reference 8. The purpose of this paper is to present the results in more detail with particular emphasis on the sources of tail buffet excitation and on the limitations of the application to horizontal tails of a buffeting analysis technique (ref. 6) which has been successfully applied to wings.

#### SYMBOLS

b span of wing or horizontal tail, ft

b' span of one wing panel outboard of strain-gage station,  
 $\frac{b}{2} - y_g$ , ft

BM static bending moment, ft-lb

c chord of wing or horizontal tail, ft

$\bar{c}$  average chord of wing or horizontal tail, ft

$C_B$  aerodynamic coefficient of buffeting intensity,

$$\sqrt{\frac{\sigma}{\omega_1^2 \frac{\pi}{2} \bar{c} \frac{M_{m1}^2}{M_1} \frac{S_1^2}{S_2} \sqrt{q}}}$$

$C_{\overline{BM}}$  static bending-moment coefficient,  $\frac{\overline{BM}}{qS'b'}$

$i_t$  angle of incidence of horizontal tail relative to body axis,  
deg

$M$  Mach number

$m$  mass per unit length of wing or horizontal tail, slugs/ft

$M_1$  a weighted mass,  $\int_{-b/2}^{b/2} m(y) [w_1(y)]^2 dy$ , slugs

$M_{m1}$  a weighted moment of mass,  $\int_{y_g}^{b/2} (y - y_g) m(y) w_1(y) dy$ ,  
ft-slugs

$q$  dynamic pressure, lb/sq ft

$R$  correlation coefficient

$S_1$  a weighted area,  $\int_{-b/2}^{b/2} c(y) w_1(y) dy$ , sq ft

$S_2$  a weighted area,  $\int_{-b/2}^{b/2} c(y) [w_1(y)]^2 dy$ , sq ft

$S'$  area of one wing panel outboard of strain-gage station,  
 $\int_{y_g}^{b/2} c(y) dy$ , sq ft

$V$  free-stream velocity, ft/sec

$w_1(y)$  mode shape of predominant buffeting mode normalized to unit deflection at tip, assumed to be  $1 - \cos \frac{\pi}{2} \frac{y}{b/2}$   
 $y$  spanwise coordinate, ft  
 $y_g$  spanwise coordinate at strain-gage station, ft  
 $\alpha$  angle of attack of body axis, deg  
 $\sigma$  root-mean-square value of buffeting bending moments measured at strain-gage station, ft-lb  
 $\omega$  natural circular frequency, radians/sec  
 $\omega_1$  natural circular frequency of predominant buffeting mode, radians/sec

Subscripts:

$_{\text{buf}}$  due to buffeting  
 $_{\text{sep}}$  due to separation  
 $_{\text{struct}}$  due to structural carry-through  
 $_{\text{turb}}$  due to turbulence

APPARATUS AND TESTS

Wind Tunnel

The model was tested in the Langley 16-foot transonic tunnel, which is a single-return wind tunnel with a slotted octagonal test section operating at atmospheric stagnation pressure. A photograph of the model sting-mounted in the test section is shown in figure 1.

Model

The configuration tested was a  $1/4$ -scale model of the X-1E airplane. This airplane is identical in exterior geometry to the original X-1-2 airplane except for a small change in the canopy and for a change in the wing. The wing is 4 percent thick, has an aspect ratio of 4, a taper ratio of 0.5, zero sweep of the  $0.4c$  line, and has NACA 65A004 modified

airfoil sections. The wing incidence is  $2^{\circ}$  with respect to the body axis. The horizontal tail is 8 percent thick, has an aspect ratio of 5, a taper ratio of 0.5, zero sweep of the 0.8c line, and has NACA 65A008 modified airfoil sections. A line drawing of the 1/4-scale model is shown in figure 2.

The model wing was designed and constructed as a true Mach number, dynamic flutter model. The dynamic characteristics of the airplane wing and aileron system were well simulated by the model. A detailed description of the model wing and a comparison with the airplane is contained in reference 10.

The dynamically scaled wing was attached to a fuselage-tail model which was designed for static aerodynamic wind-tunnel tests. The fuselage was constructed of heavily reinforced magnesium alloy. The rear  $5\frac{1}{2}$  inches of the model fuselage was omitted because of space limitations. The vertical tail was solid aluminum alloy and the horizontal tail was solid steel with several holes drilled in the spanwise direction.

The model and full-scale natural frequencies of modes involving significant motions of the wing and horizontal tail are tabulated in table I for comparable conditions of restraint. As might be expected, the natural frequencies for the dynamically scaled model wing agree very well with those for the airplane wing; however, the frequencies for the geometrically scaled horizontal tail do not agree very well with those for the airplane. Some of the consequences of the disagreement in frequencies of the horizontal tail will be discussed subsequently.

#### Instrumentation

The wing data presented in this paper were obtained by using a bending strain-gage bridge which was mounted on the right wing panel near the elastic axis 0.21 foot outboard of the wing-fuselage juncture. The horizontal-tail data were obtained by using a bending strain-gage bridge mounted on the left horizontal-tail panel near the elastic axis and 0.15 foot outboard of the center line. These strain-gage locations are illustrated in figure 2. Static calibrations indicated that the strain-gage bridges on both the wing and horizontal tail were excellent indicators of bending moment, i.e., there was very little sensitivity to loadings other than bending moments.

The strain-gage signals were amplified and recorded on a 14-channel magnetic tape recorder utilizing a frequency modulation system. In order to obtain root-mean-square (rms) and power-spectral-density information, the tape records were played back after the conclusion of the

tests into analog data-reduction equipment described in reference 11. The static bending moment acting on the wing was obtained by switching the strain-gage bridge signal from the tape recorder to a self-balancing potentiometer.

#### Test Procedure

Before each test, calibration records were obtained to minimize the effects of small changes in amplifier sensitivities. After this procedure had been completed, the model was set at  $\alpha = 0^\circ$  and the tunnel speed was increased to the desired Mach number. At Mach numbers of 0.40, 0.50, 0.60, 0.70, 0.75, and 0.80, tape records of approximately 45 seconds duration were obtained for angles of attack between  $-2^\circ$  and  $15^\circ$ . At Mach numbers of 0.85 and 0.90, the maximum angles of attack were limited to  $14^\circ$  and  $7^\circ$ , respectively, by the allowable loads on the model wing. In addition, data were obtained at angles of attack down to  $-15^\circ$  at  $M = 0.40$ .

Most of the tests were made with the horizontal tail set at an angle of incidence of  $2^\circ$ ; however, some tests at  $M = 0.40$  were made with the angle of incidence at  $-2^\circ$  and  $3.5^\circ$ .

#### METHOD OF ANALYSIS

The successful application of the methods of generalized harmonic analysis to the wing buffeting problem in the form of a relatively simple wind-tunnel technique has led to the hope that the same technique might be applied to the problem of estimating buffeting loads on the horizontal tail. One of the purposes of the present investigation was to determine the feasibility of applying this technique, developed for wings, to the case of the horizontal tail.

The wind-tunnel technique that has evolved from the application of generalized harmonic analysis to the buffeting problem is based on the assumption that buffeting can be treated as a Gaussian random process involving the linear response of a lightly damped single-degree-of-freedom elastic system. If it is further assumed that the damping of the system is entirely aerodynamic, the following expression relates the root-mean-square buffeting bending moments to the physical characteristics of the surface, its operating conditions, and an aerodynamic coefficient of buffeting intensity which will be referred to herein as a "buffet coefficient":

$$\sigma = \sqrt{\omega_1^2 \frac{\pi}{2} \bar{c} \frac{M_{m1}^2}{M_1} \frac{S_1^2}{S_2^2} \sqrt{q} C_B} \quad (1)$$

Equation (1) was first presented in a slightly different form in reference 6 and has been developed more fully in reference 12. The quantities under the first radical represent the physical constants of the model, values of which are presented in table II. In this investigation, the root-mean-square bending moment  $\sigma$  was measured near the root of the wing and the horizontal tail. The data were reduced to a nondimensional buffet coefficient  $C_B$  by rearranging the expression given by equation (1). Thus,

$$C_B = \frac{\sigma}{\sqrt{\omega_1^2 \frac{\pi}{2} \bar{c} \frac{M_{m1}^2}{M_1} \frac{S_1^2}{S_2^2} \sqrt{q}}} \quad (2)$$

The buffet coefficient  $C_B$  defined in this manner represents a nondimensional aerodynamic coefficient of buffet intensity. It is, in essence, a coefficient of the ratio of the aerodynamic driving force to the aerodynamic damping force.

The frequency  $\omega_1$  chosen for use in this expression was the natural frequency (from still-air vibration tests) of the most predominant mode of response during buffeting. Typical bending-moment output spectra for the model wing and horizontal tail are shown in figure 3. The predominant mode of response for both the wing and the horizontal tail is the symmetric bending mode. Some response is noted in other modes for both the wing and horizontal tail; however, these additional modes represent a small part of the total response.

For an indication of static loading conditions, the wing static bending-moment coefficient was measured and is defined by the following relation:

$$C_{\overline{BM}} = \frac{\overline{BM}}{qS'b'}$$

where  $\overline{BM}$  is the mean value of the bending moment measured on one panel and  $S'$  and  $b'$  are the panel area and span, respectively, outboard of the strain-gage station.

## RESULTS AND DISCUSSION

The basic quantities measured in this investigation are presented in figure 4 in the form of curves of the nondimensional buffet coefficient  $C_B$  for both the wing and the horizontal tail as functions of angle of attack for Mach numbers from 0.40 to 0.90. As stated previously, the buffet coefficient  $C_B$  is a nondimensional aerodynamic coefficient of buffeting intensity and represents the ratio of the aerodynamic driving force to the aerodynamic damping force. For reference purposes, the wing static bending-moment coefficients  $C_{BM}$  are shown in the same figure.

Comparison of Buffet Loads on Wing and  
Horizontal Tail of Model

Examination of figure 4 indicates that the buffet coefficients for both the wing and the tail of the model have somewhat similar characteristics throughout the Mach number range. The buffet coefficients are relatively constant over the lower range of angle of attack and then increase more or less abruptly at angles of attack corresponding to the buffet boundary. The response of the model in the lower range of angle of attack is believed to be due primarily to residual tunnel turbulence and must be interpreted as a source of error or uncertainty in the experiments. For example, a low intensity buffet might occur at low lift conditions without being detected because of the continuous response of the model to the tunnel turbulence. It is difficult to assess the effects of the response to turbulence on the true buffet data, and for that reason no attempt has been made to extract the response due to turbulence as a tare from the basic data shown in figure 4.

Since the buffeting loads have been reduced to a nondimensional coefficient, it is possible to discuss the relative intensity of buffeting on the wing and the horizontal tail. At low angles of attack the buffet coefficients for the horizontal tail are about half as large as those for the wing. This result may be due to several effects. For example, it seems reasonable to assume that both the wing and the tail are being excited by the tunnel turbulence, but the horizontal tail is operating in a field of turbulence which has been smoothed by the wing in much the same manner as the downwash of the wing reduces the steady-state angle of attack of the horizontal tail.

Beyond the buffet boundary, for most of the Mach numbers investigated, the buffet coefficients for the wing tend to reach a maximum

value within the range of angle of attack covered. The buffet coefficients for the horizontal tail, however, continue to increase up to the maximum angles tested for most Mach numbers. (See fig. 4.) The maximum buffet coefficients reached for the horizontal tail are about twice as large as those for the wing; however, this ratio tends to decrease with increasing Mach number. This result is in qualitative agreement with flight measurements for other airplanes which have indicated that horizontal-tail buffeting loads are usually a larger percentage of the design load than are the buffeting loads on the wing. The larger buffeting loads experienced by the horizontal tail are usually attributed to the effect of the wing wake. Some studies of the sources of buffeting of the horizontal tail will be discussed subsequently; however, it would seem appropriate to consider first the degree to which the model simulated the significant dynamic characteristics of the airplane.

#### Comparison of Buffeting Loads on Model and Airplane

Wing.- It has been pointed out (refs. 6 and 8) that one essential requirement for model simulation in buffeting studies is that the model should respond during buffeting in the same mode as the airplane. This similarity of response is illustrated in figure 5, where typical spectra of bending-moment output during buffeting are compared for the wing of the 1/4-scale model and of the airplane. The spectra are shown in terms of the reduced frequency and it can be seen that both the airplane and the model respond at essentially the same value of this parameter. Although some response is noted at other frequencies, most of the total response is associated with the symmetric bending mode.

As discussed in reference 8, the presence of wind-tunnel turbulence complicates the interpretation of buffet data. In principle, the effects of turbulence on the measured buffeting loads may be extracted as a tare. In practice, however, this extraction requires knowledge of or an assumption regarding a complicated mechanism. The loads due to turbulence and buffeting are related to the total measured load by the following expression:

$$\sigma_{\text{total}}^2 = \sigma_{\text{turb}}^2 + 2R\sigma_{\text{turb}}\sigma_{\text{buf}} + \sigma_{\text{buf}}^2 \quad (3)$$

where  $R$  is a correlation coefficient which expresses the degree of interrelation between the loads due to turbulence and the loads due to buffeting. The correlation coefficient may have values from -1 to 1. If the two random processes associated with turbulence and with buffeting are completely independent and uncorrelated,  $R$  is equal to 0 and the buffeting load is

$$\sigma_{buf} = \sqrt{\sigma_{total}^2 - \sigma_{turb}^2} \quad (4)$$

If, on the other hand, it is assumed that the two processes are in phase,  $R$  is equal to 1 and the buffeting load is

$$\sigma_{buf} = \sigma_{total} - \sigma_{turb} \quad (5)$$

Very little evidence exists concerning the correlation between loads due to turbulence and those due to buffeting and, consequently, some assumption regarding the value of  $R$  is required if it is desired to extrapolate model data containing an appreciable portion of loads due to turbulence to flight conditions.

In the present investigation, the agreement between model and airplane buffeting loads has been examined for both  $R = 0$  and  $R = 1$ . Inspection of figure 6 indicates that good agreement is obtained for the case where  $R$  is taken as 1. The extent of the comparison is limited by the small range of flight conditions available for comparison. It should be noted that the use of the difference in rms values as a means of eliminating the loads due to turbulence has not been clearly established by this single comparison. The best solution to this problem in future studies would be to use a wind tunnel with a very low turbulence level.

Horizontal tail.— The natural frequencies of modes involving appreciable motions of the wing and the horizontal tail are presented in table I for the 1/4-scale model and are compared with the scaled frequencies of the same modes for the airplane. The agreement in frequencies for the model and the airplane wing is considered to be good; however, the frequencies of the horizontal tail are quite dissimilar except for the symmetric bending mode. These large differences in natural frequencies for the horizontal tail would be expected to lead to large differences in the dynamic characteristics of the buffeting response. These expectations are confirmed by the data shown in figure 7, which compares the power spectra of buffeting loads acting on the horizontal tail of the airplane and the 1/4-scale model. This comparison, which has been shown before in reference 8, indicates that the predominant buffeting mode for the airplane was the fuselage torsion mode whereas that for the model was the symmetric horizontal-tail bending mode. With such large differences in the character of the buffeting response, it would not be expected that the model data could be used for quantitative estimates of full-scale horizontal-tail buffeting loads. Furthermore, it would appear that in order to make wind-tunnel measurements of horizontal-tail buffeting loads for purposes of extrapolation to flight conditions, it would be necessary to use a model which was dynamically scaled in such a way that the dynamic characteristics of the rearward portion of

the fuselage as well as the empennage simulated the characteristics of the airplane. It appears that a true Mach number flutter model would meet these requirements.

#### Sources of Buffeting of Horizontal Tail

Recognizing the limitations of the 1/4-scale model used in this investigation, it was still considered possible to obtain some qualitative information of interest concerning the relative contributions of various sources of buffeting of the horizontal tail. The sources of buffeting loads considered were those due to (1) wing wake, (2) separation on the tail itself, and (3) structural carry-through from the wing to the fuselage to the horizontal tail. In addition, some of the measured load was due to the residual turbulence in the tunnel and must be considered as a tare to be removed from the data.

A similar resolution of the sources of horizontal-tail buffeting was suggested by Luskin and Lapin (ref. 13), along with some suggestions regarding experimental techniques for determining the separate contributions of the various sources. For example, it was suggested that the effect of the wing wake could be deduced from model tests with and without the wing. In the present investigation it was not practical to test without the wing because the wing was essentially an integral part of the sting attachment fitting. Consequently, in order to obtain an estimate of the effect of the wing wake, tests were conducted at high negative angles of attack so that the horizontal tail was well removed from the wing wake. At high negative angles of attack the part of the horizontal-tail buffeting loads due to the wing wake was assumed to be zero. In order to obtain an estimate of the part of the horizontal-tail buffeting loads due to separation on the horizontal tail, tests were conducted with the horizontal tail set at various angles of incidence. In this manner, it was possible to cause the flow to separate on the horizontal tail at angles of attack well below that at which wing buffeting began. Finally, the part of the buffeting load due to structural carry-through was deduced by subtracting the part due to separation from the total measured load at negative angles of attack where the part due to wing wake was not present.

A qualitative measure of the contribution of these various sources of buffeting can be obtained by examination of the data shown in figure 8 where the measured values of the root-mean-square bending moments acting at the strain-gage station for both the wing and horizontal tail are shown as functions of angle of attack (relative to the fuselage center line) for various incidence angles on the horizontal tail. Examination of figure 8 indicates that the buffeting loads acting on the wing are relatively symmetrical about the angle of attack corresponding to zero lift on the wing, namely,  $\alpha = -2^\circ$ . In contrast, the buffeting loads on the

horizontal tail are much smaller at negative angles of attack than they are at positive angles. This is interpreted to mean that the wing wake causes a large part of the total buffeting load on the horizontal tail and that separation on the tail and structural carry-through effects are relatively small.

In order to obtain a quantitative estimate of the relative contributions of the various sources, it is necessary to have some expression relating the various sources to the total load. The analytical development of such an expression which could be expected to apply generally for a variety of configurations and conditions is beyond the scope of this paper. However, an expression has been used to represent this presumably complicated relationship which has justification in its simplicity if not its rigor.

If it is assumed that the various sources of buffeting load act as individual uncorrelated time variables, then the square of the total fluctuating load can be expressed as the sum of the squares of the individual parts. This leads to the following expression:

$$\sigma_{\text{total}}^2 = \sqrt{\sigma_{\text{wake}}^2 + \sigma_{\text{sep}}^2 + \sigma_{\text{struc}}^2 + \sigma_{\text{turb}}^2} \quad (6)$$

It could be argued, for example, that the load due to the wing wake and due to separation on the tail might be correlated because of a possible "triggering" action of the wake on the boundary layer of the tail. However, such a detailed examination of the mechanism of buffeting of the horizontal tail is beyond the scope of this investigation and for the present purpose it is believed that equation (6) is adequate.

With the use of equation (6) and the data shown in figure 8, the parts of the total buffeting load due to the various sources were determined by the following procedure: At negative angles of attack, after the loads due to turbulence have been extracted as a tare, the total measured load may be considered to be the sum of the parts due to separation on the tail and structural carry-through. Furthermore, by testing at two different angles of incidence of the horizontal tail, the separate effects of these two sources can be determined for a small range of geometric angle of attack of the horizontal tail. It should be pointed out that the use of the geometric angle of attack of the tail is a simplifying assumption which ignores the downwash effects of the wing. However, it is believed that in the present case a more complete analysis, including downwash effects, would lead to essentially the same results. Figure 9 indicates that at  $i_t = -2^\circ$  wing buffeting starts at a geometric angle of the horizontal tail of  $-10^\circ$ . Consequently, the buffeting of the tail below this angle can be considered to represent the small part due to

separation on the tail. For  $i_t = 3.5^\circ$  wing buffeting starts at about the same geometric angle as that corresponding to separation on the tail; thus, the load due to structural carry-through can be obtained by subtracting the load due to separation on the tail. The loads associated with these two sources of buffeting are shown in figure 10 as functions of the increment in geometric angle of attack beyond the start of buffeting. At positive angles of attack, the sum of these two loads can be subtracted from the total buffeting load to give an indication of the part of the load due to the wing wake.

By following this procedure, the parts of the total buffeting load due to the various sources of buffeting have been plotted in figure 11 as a function of angle of attack for  $M = 0.4$  and  $i_t = 2^\circ$ . Presentation of these results in a manner that is not misleading is difficult. In figure 11 the various components of bending moment are plotted in the squared form; that is, they have units of (foot-pounds)<sup>2</sup>. Presented in this form the sum of the various components is equal to the total buffeting load and it appears that at  $\alpha = 10^\circ$ , for example, almost 90 percent of the buffeting of the horizontal tail is due to the wing wake. This numerical result indicates that removal of the wing wake would reduce the rms bending moments to about one-third the original value  $(\sqrt{1 - 0.9} \approx \frac{1}{3})$ . This result is in qualitative agreement with the data shown in figure 8.

#### CONCLUDING REMARKS

The buffeting loads acting on the wing and horizontal tail of a 1/4-scale model of the X-1E airplane have been measured in the Langley 16-foot transonic tunnel in the Mach number range from 0.40 to 0.90. When the buffeting loads were reduced to a nondimensional aerodynamic coefficient of buffeting intensity, it was found that the maximum buffeting intensity of the horizontal tail was about twice as large as that of the wing. Comparison of power spectra of buffeting loads acting on the horizontal tail of the airplane and of the model indicated that the horizontal tail of the model, which was of conventional force-test-model design, responded in an entirely different mode than did the airplane. This result implied that if quantitative extrapolation of model data to flight conditions were desired, a dynamically scaled model of the rearward portion of the fuselage and empennage would be required.

A study of the sources of horizontal-tail buffeting of the model indicated that the wing wake contributed a large part of the total

buffeting load. At one condition it was found that removal of the wing wake would reduce the buffeting loads on the horizontal tail to about one-third of the original value.

Langley Aeronautical Laboratory,  
National Advisory Committee for Aeronautics,  
Langley Field, Va., June 20, 1958.

## REFERENCES

1. Liepmann, H. W.: An Approach to the Buffeting Problem From Turbulence Considerations. Rep. No. SM-13940, Douglas Aircraft Co., Inc., Mar. 13, 1951.
2. Liepmann, H. W.: On the Application of Statistical Concepts to the Buffeting Problem. Jour. Aero. Sci., vol. 19, no. 12, Dec. 1952, pp. 793-800, 822.
3. Liepmann, H. W.: Parameters for Use in Buffeting Flight Tests. Rep. No. SM-14631, Douglas Aircraft Co., Inc., Jan. 3, 1953.
4. Huston, Wilber B., and Skopinski, T. H.: Measurement and Analysis of Wing and Tail Buffeting Loads on a Fighter Airplane. NACA Rep. 1219, 1955. (Supersedes NACA TN 3080.)
5. Huston, Wilber B., and Skopinski, T. H.: Probability and Frequency Characteristics of Some Flight Buffet Loads. NACA TN 3733, 1956.
6. Huston, Wilber B., Rainey, A. Gerald, and Baker, Thomas F.: A Study of the Correlation Between Flight and Wind-Tunnel Buffeting Loads. NACA RM L55E16b, 1955.
7. Kemp, William B., Jr., and King, Thomas J., Jr.: Wind-Tunnel Measurements of Wing Buffeting on 1/16-Scale Model of Douglas D-558-II Research Airplane. NACA RM L56G31, 1956.
8. Davis, Don D., Jr., and Huston, Wilber B.: The Use of Wind Tunnels to Predict Flight Buffet Loads. NACA RM L57D25, 1957.
9. Davis, Don D., Jr., and Wornom, Dewey B.: Buffet Tests of an Attack-Airplane Model With Emphasis on Analysis of Data From Wind-Tunnel Tests. NACA RM L57H13, 1958.
10. Gibson, Frederick W., Igoe, William B., and Maloney, P. R.: Experimental Investigation of Wing-Aileron Flutter Characteristics of a 1/4-Scale Dynamic Model of the X-1E Airplane. NACA RM L57E15, 1957.
11. Smith, Francis B.: Analog Equipment for Processing Randomly Fluctuating Data. Aero. Eng. Rev., vol. 14, no. 5, May 1955, pp. 113-119.
12. Huston, Wilber B.: A Study of the Correlation Between Flight and Wind-Tunnel Buffet Loads. Presented to Structures and Materials Panel of AGARD (Copenhagen, Denmark), April 29 - May 4, 1957.

13. Luskin, Harold, and Lapin, Ellis: An Analytical Approach to the Fuel Sloshing and Buffeting Problems of Aircraft. Rep. No. SM-14068, Douglas Aircraft Co., Inc., June 27, 1951.

TABLE I.- COMPARISON OF NATURAL FREQUENCIES FOR THE WING  
AND EMPENNAGE OF THE FULL-SCALE AND

$\frac{1}{4}$  - SCALE X-1E AIRPLANE

Mode	Frequency, cps, for -	
	Full-scale airplane (a)	$\frac{1}{4}$ - scale model
Wing:		
Symmetric first bending . . . . .	32.4	<sup>b</sup> 36.5
Antisymmetric first bending . . . . .	62	76 to 79
Antisymmetric first torsion . . . . .	114	123 to 125
Symmetric first torsion . . . . .	142	136.5
Empennage:		
Vertical-tail bending . . . . .	120	49
Fuselage torsion . . . . .	44	60
Symmetric horizontal-tail bending . . . . .	110	<sup>c</sup> 112

<sup>a</sup>Frequencies listed for airplane have been multiplied by 4 to make them directly comparable to model values.

<sup>b</sup>Structural damping coefficient is 0.007.

<sup>c</sup>Structural damping coefficient is 0.003.

TABLE II.- PHYSICAL CONSTANTS FOR THE MODEL

WING AND HORIZONTAL TAIL

	Wing	Horizontal tail
$\omega_1$ , radians/sec . . . . .	226	703
$\bar{c}$ , ft . . . . .	1.429	0.5724
$M_{m1}$ , ft-slugs . . . . .	0.1997	0.0662
$M_1$ , slugs . . . . .	0.1641	0.0972
$S_1$ , sq ft . . . . .	2.48	0.499
$S_2$ , sq ft . . . . .	1.45	0.292
$\sqrt{\omega_1^2 \frac{\pi}{2} \bar{c} \frac{M_{m1}^2}{M_1} \frac{S_1^2}{S_2^2}}, \text{ ft}^2 \text{-lb}^{1/2} . . . . .$	344	130.9

CONFIDENTIAL

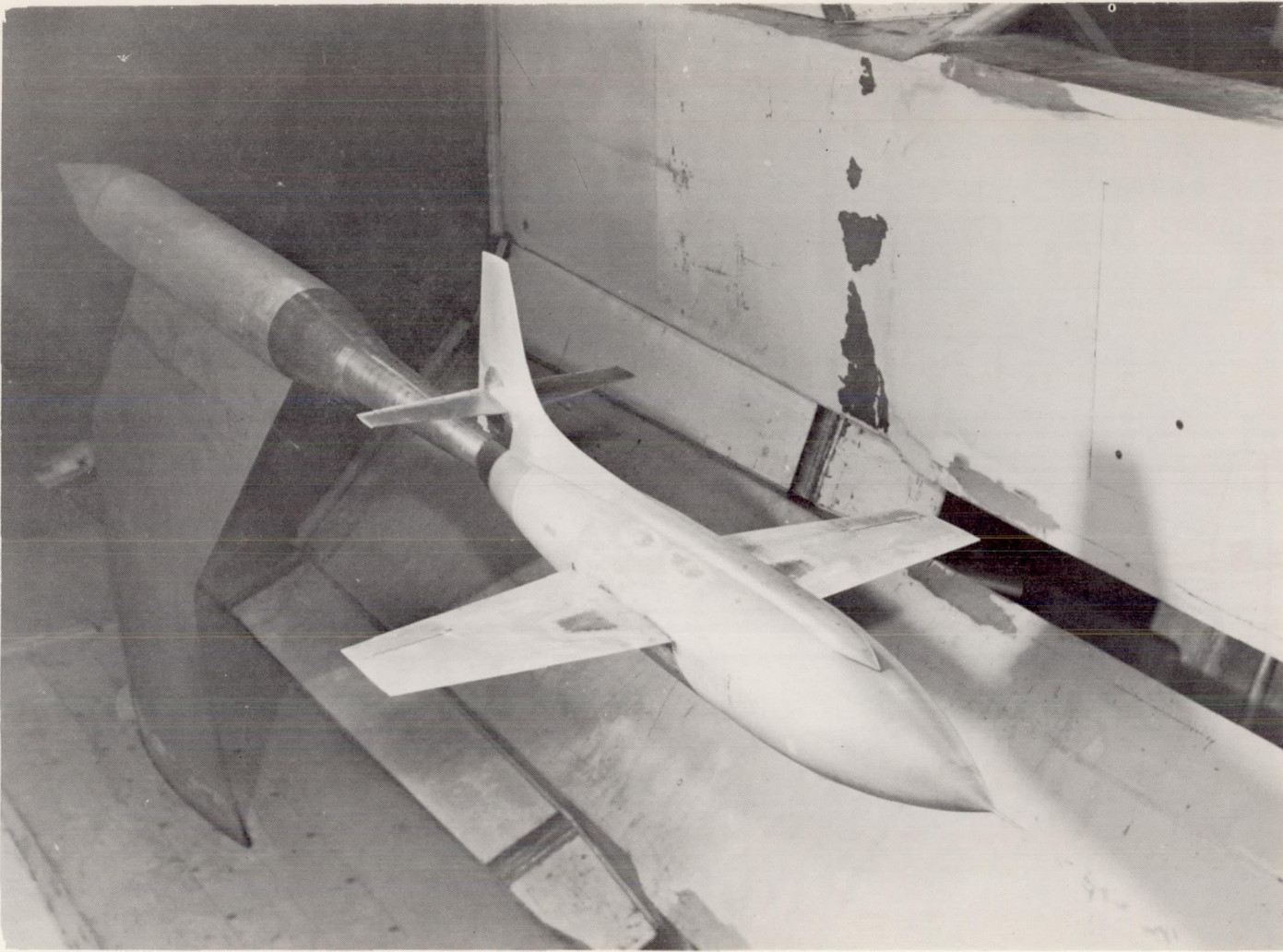


Figure 1.- One-fourth scale model of X-1E airplane mounted on the sting in the Langley 16-foot transonic tunnel.

L-91172

NACA RM L58F25

CONFIDENTIAL

18

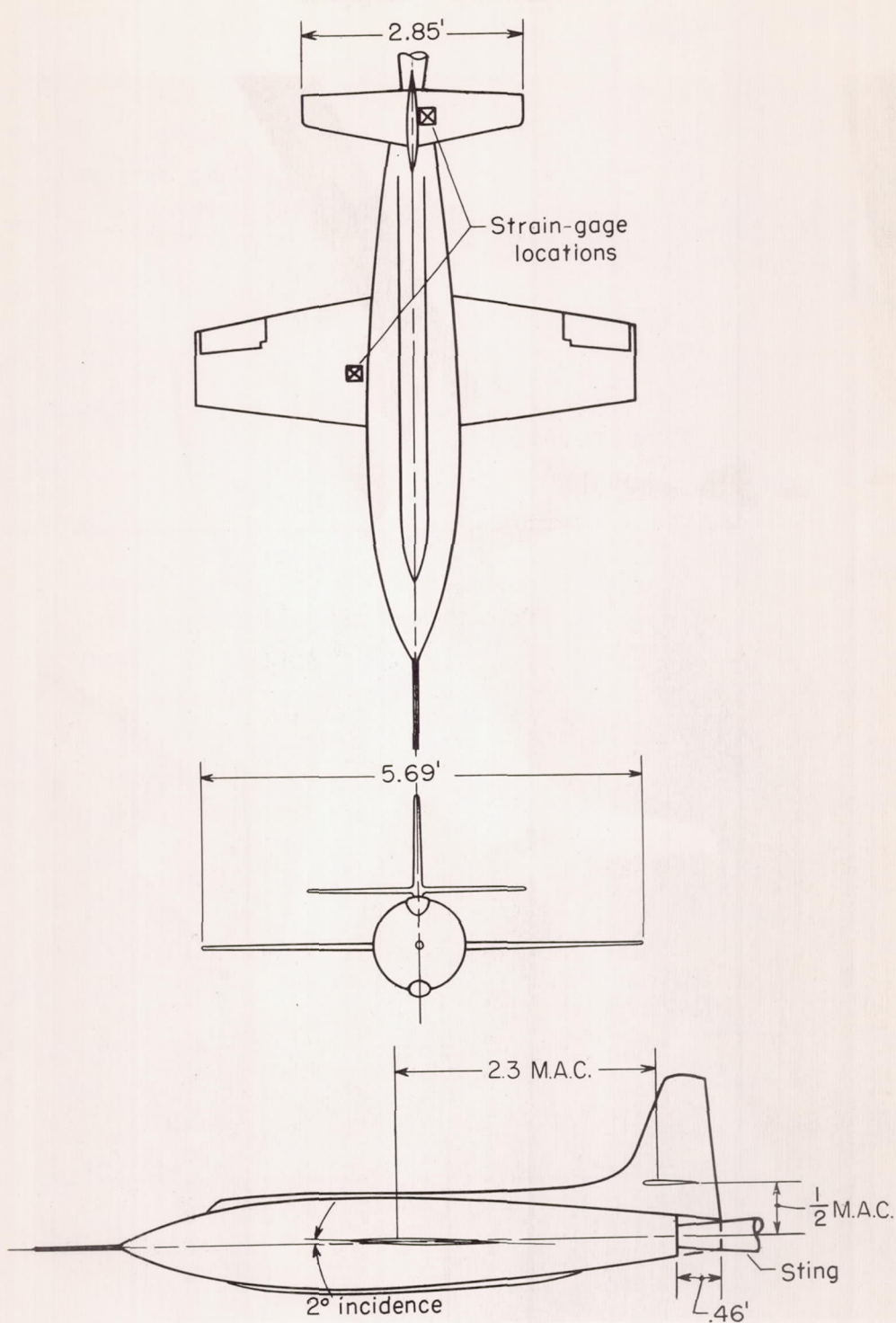


Figure 2.- Line drawing of model.

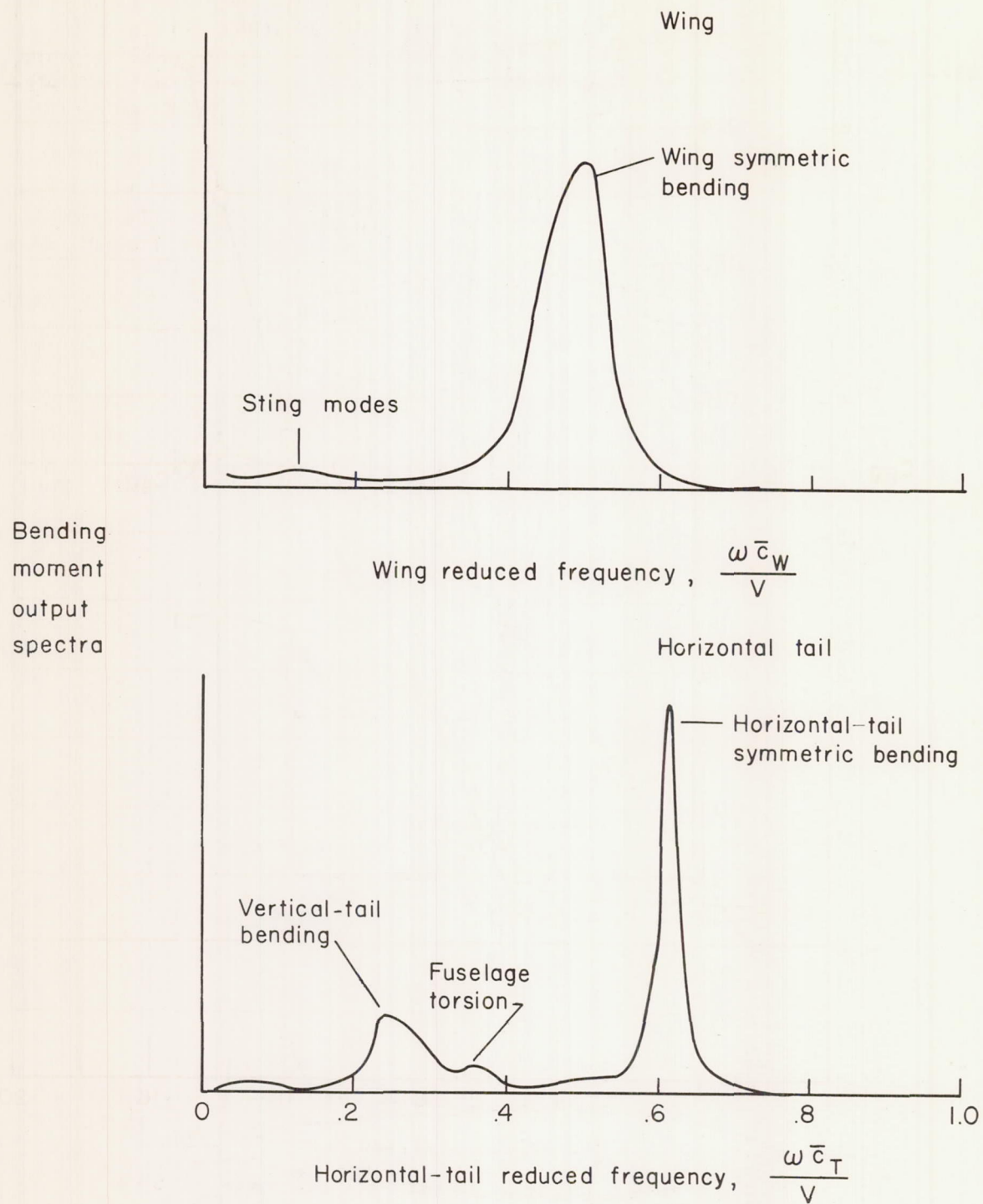
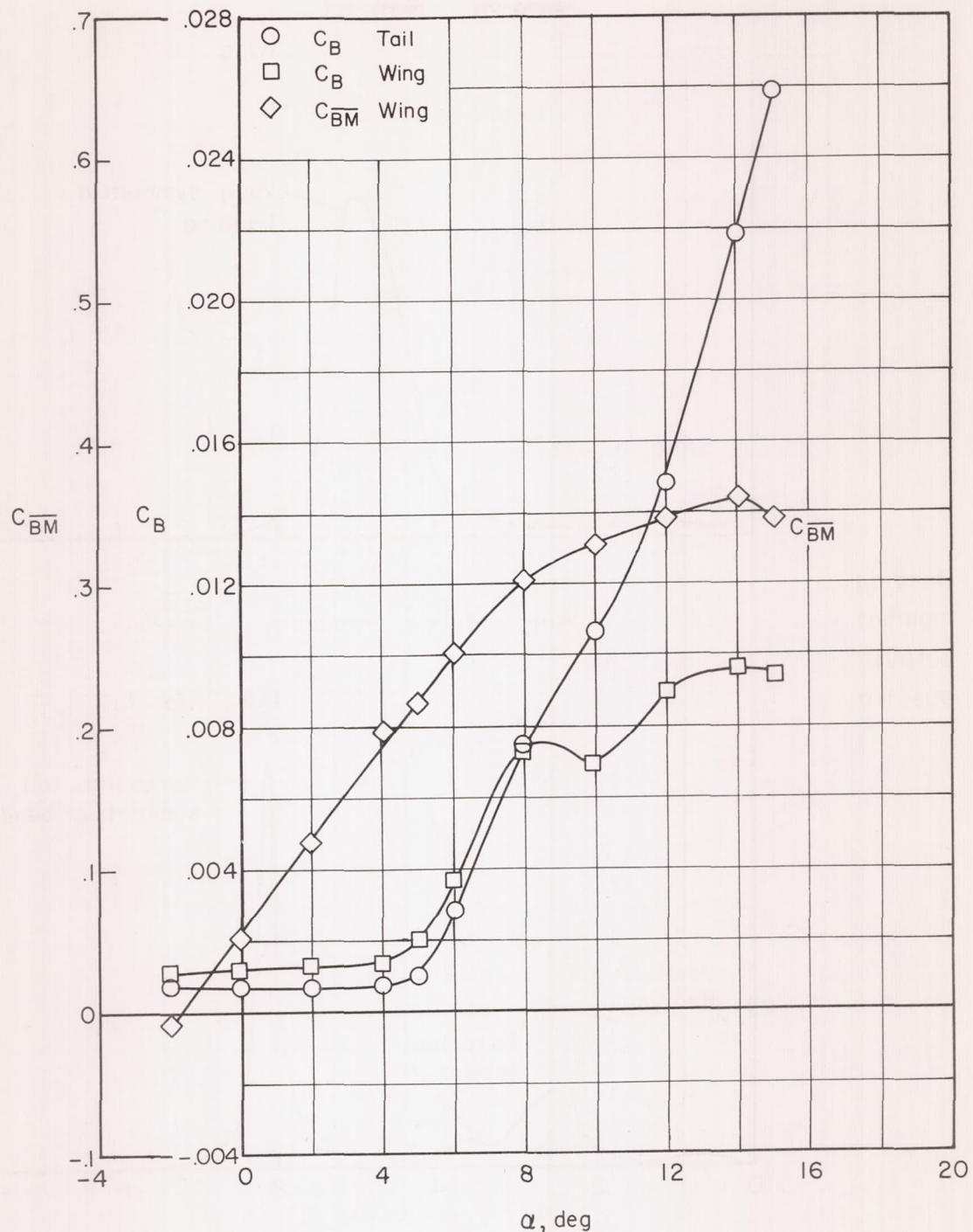
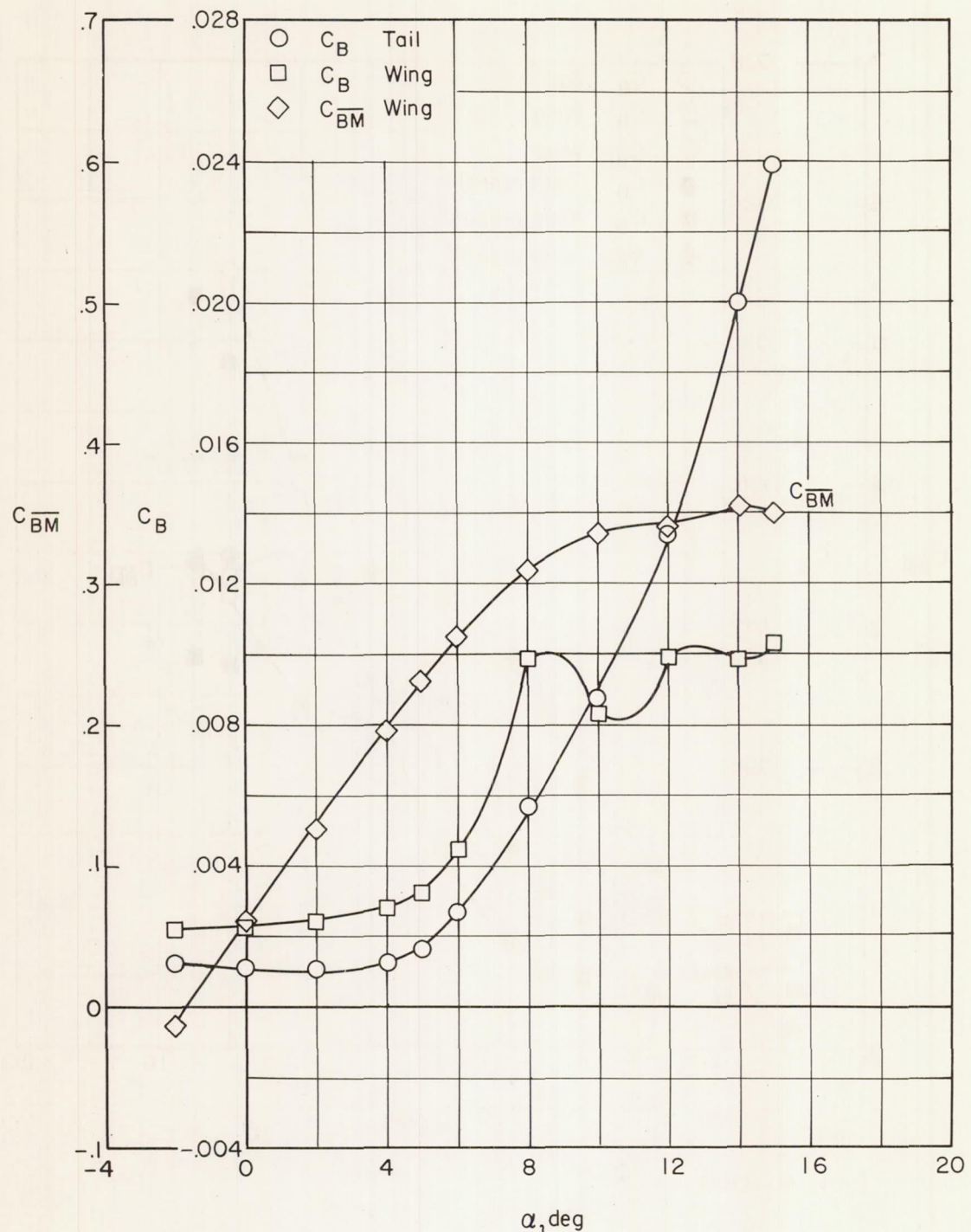


Figure 3-- Typical power spectra of bending moment during buffeting of 1/4-scale model.



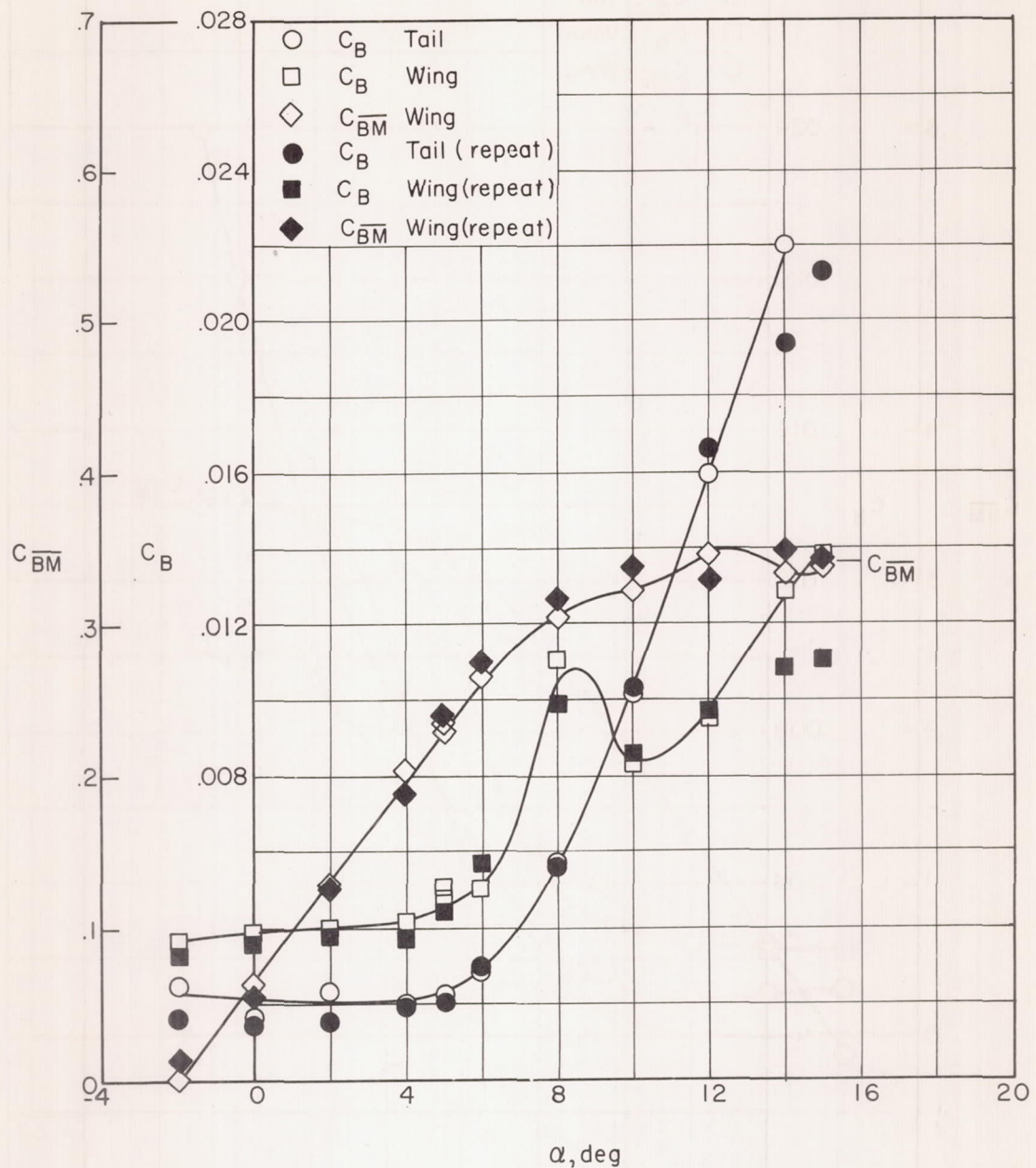
(a)  $M = 0.40$ .

Figure 4.- Variation of buffet coefficient and static bending-moment coefficient with angle of attack.  $i_t = 2^\circ$ .



(b)  $M = 0.50$ .

Figure 4.- Continued.



(c)  $M = 0.60$ .

Figure 4.- Continued.

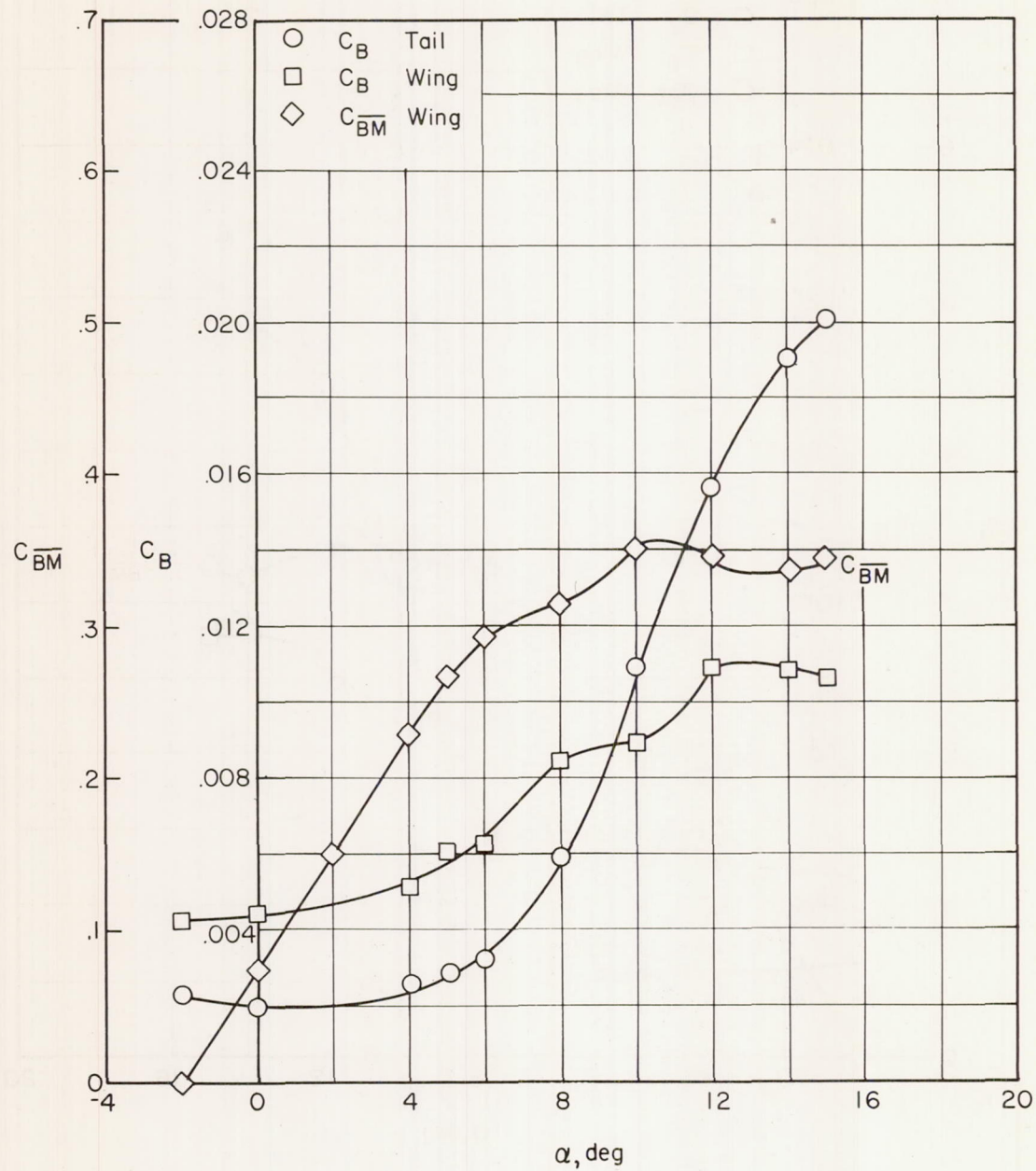
(d)  $M = 0.70$ .

Figure 4.- Continued.

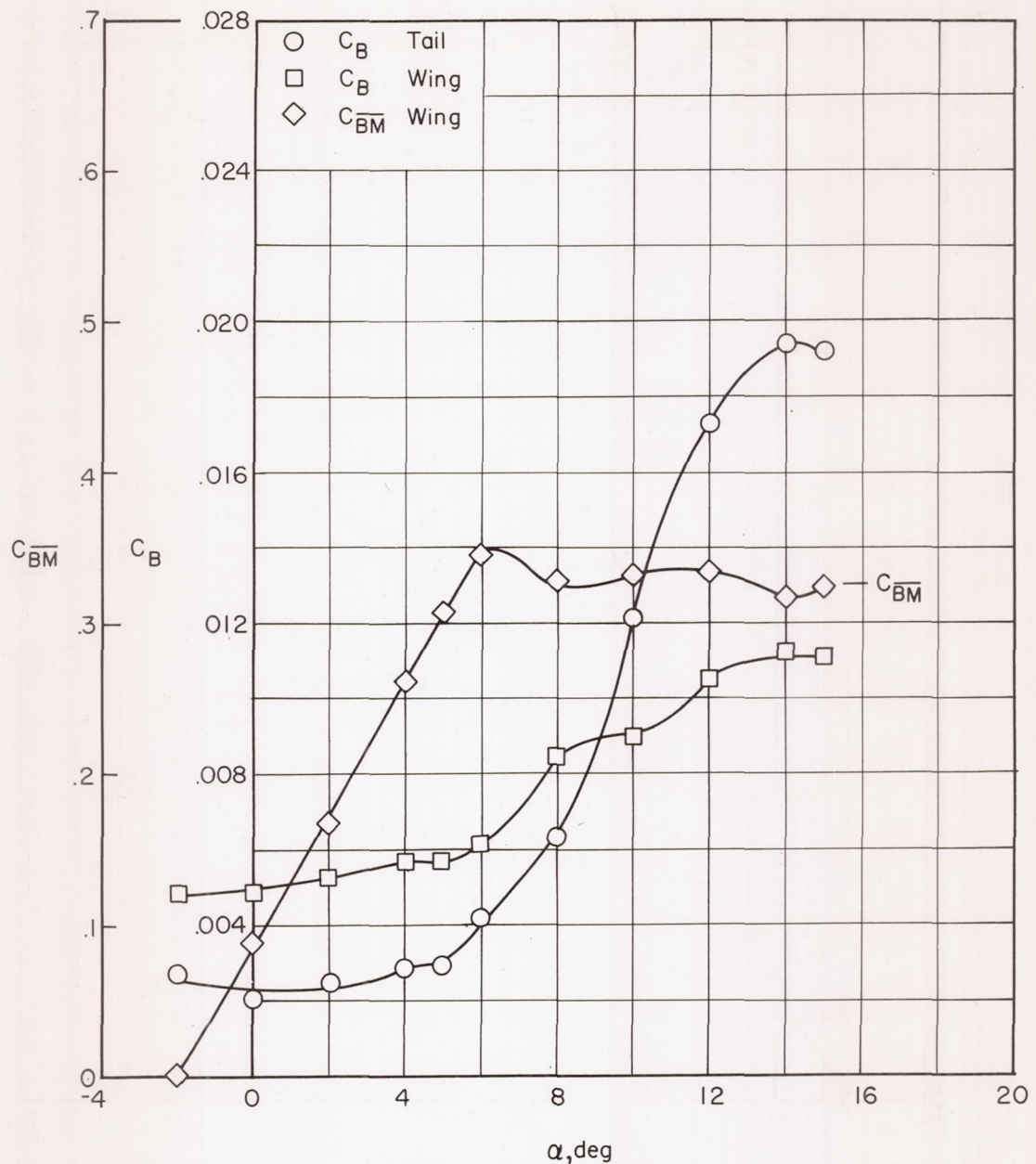
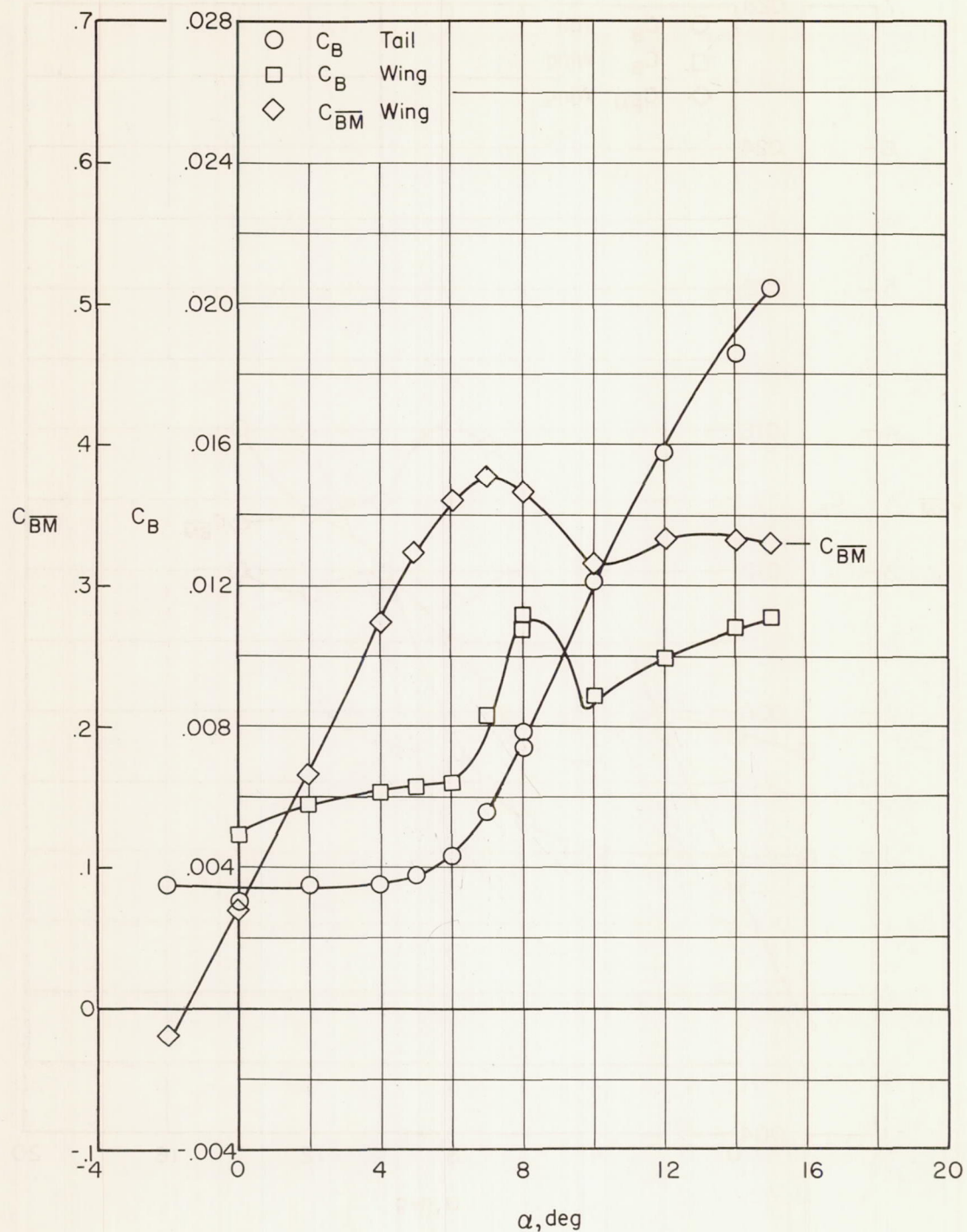
(e)  $M = 0.75$ .

Figure 4.- Continued.



(f)  $M = 0.80$ .

Figure 4.- Continued.

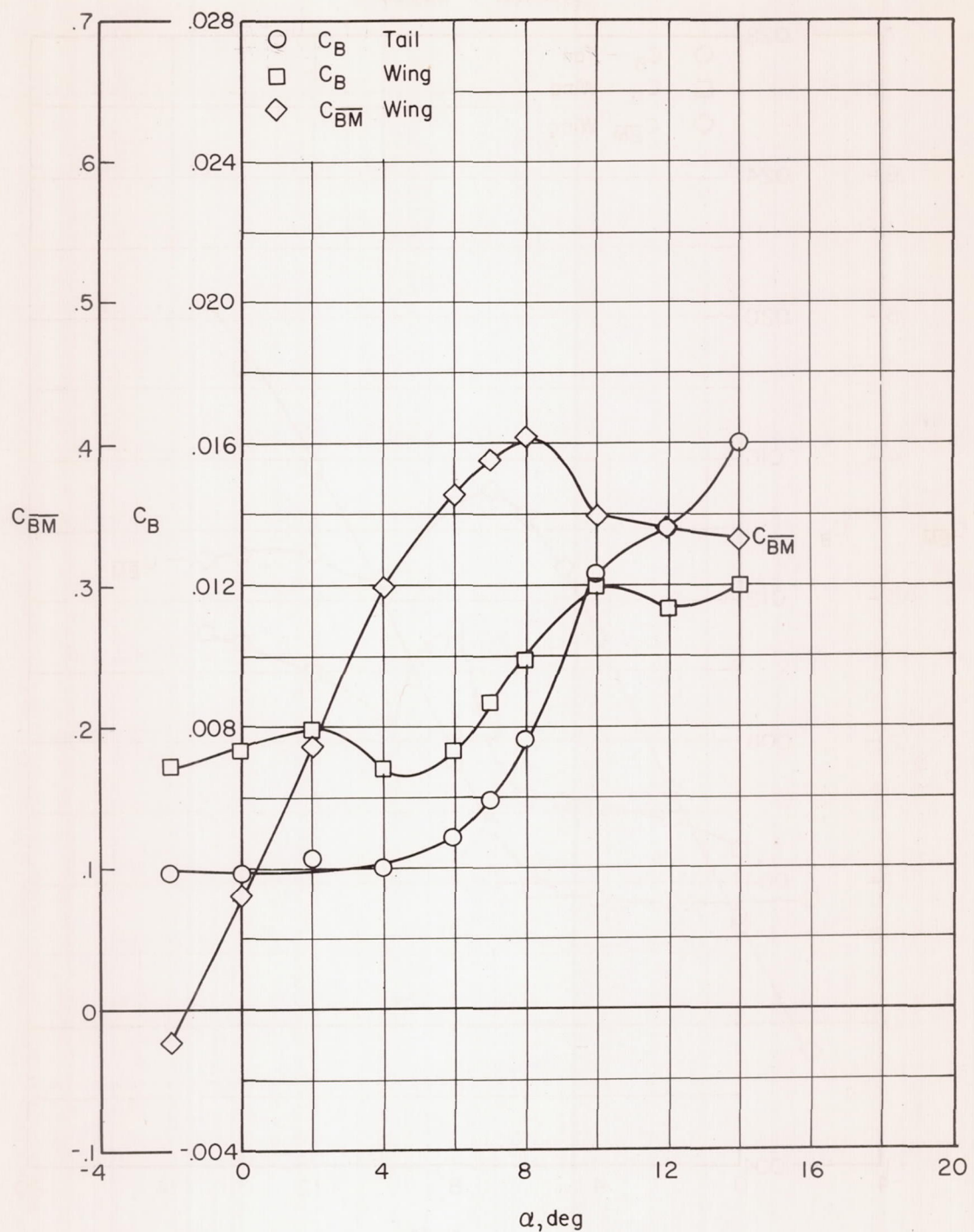
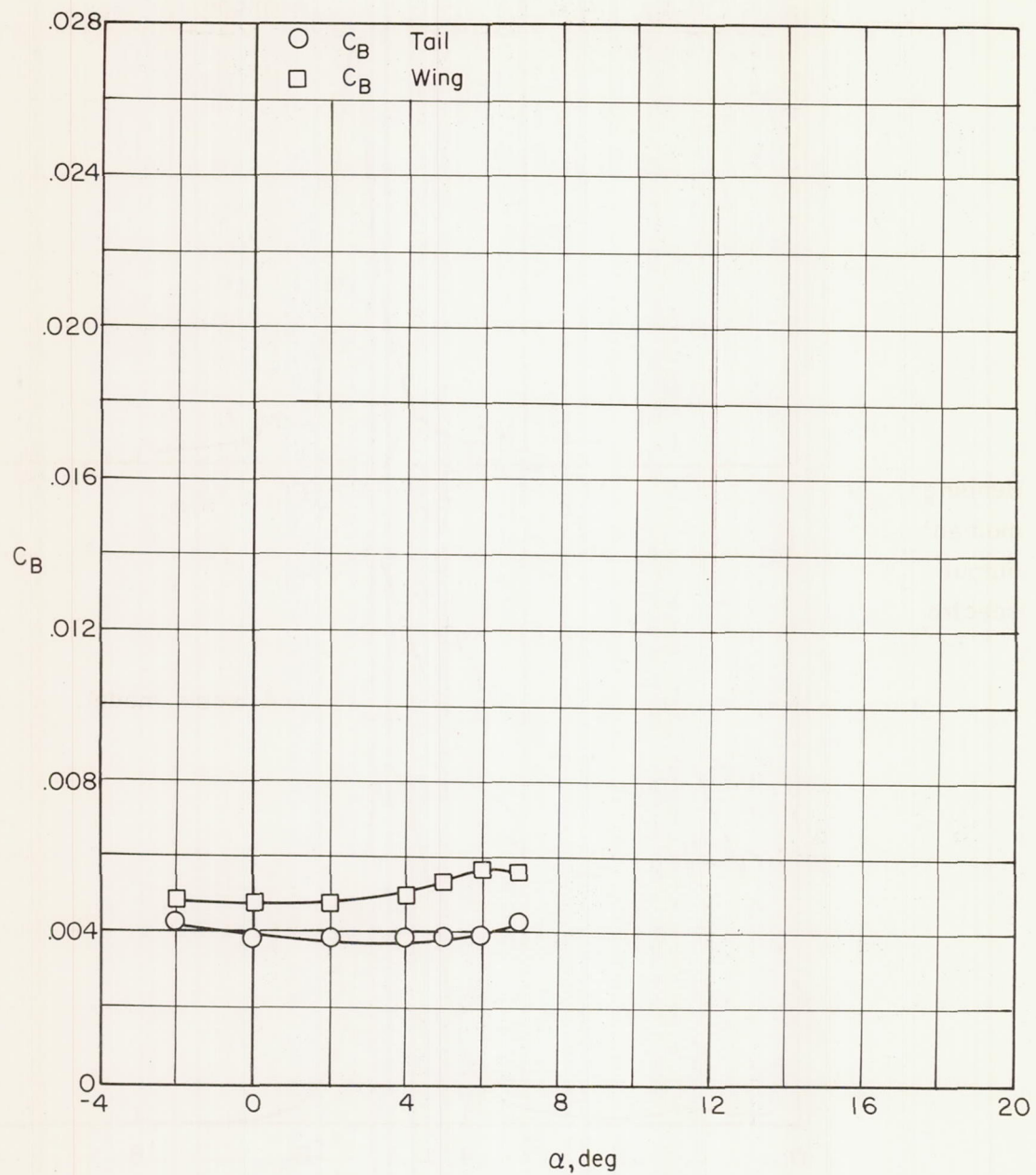
( g )  $M = 0.85$ .

Figure 4.- Continued.



( h )  $M = 0.90$ .

Figure 4.- Concluded.

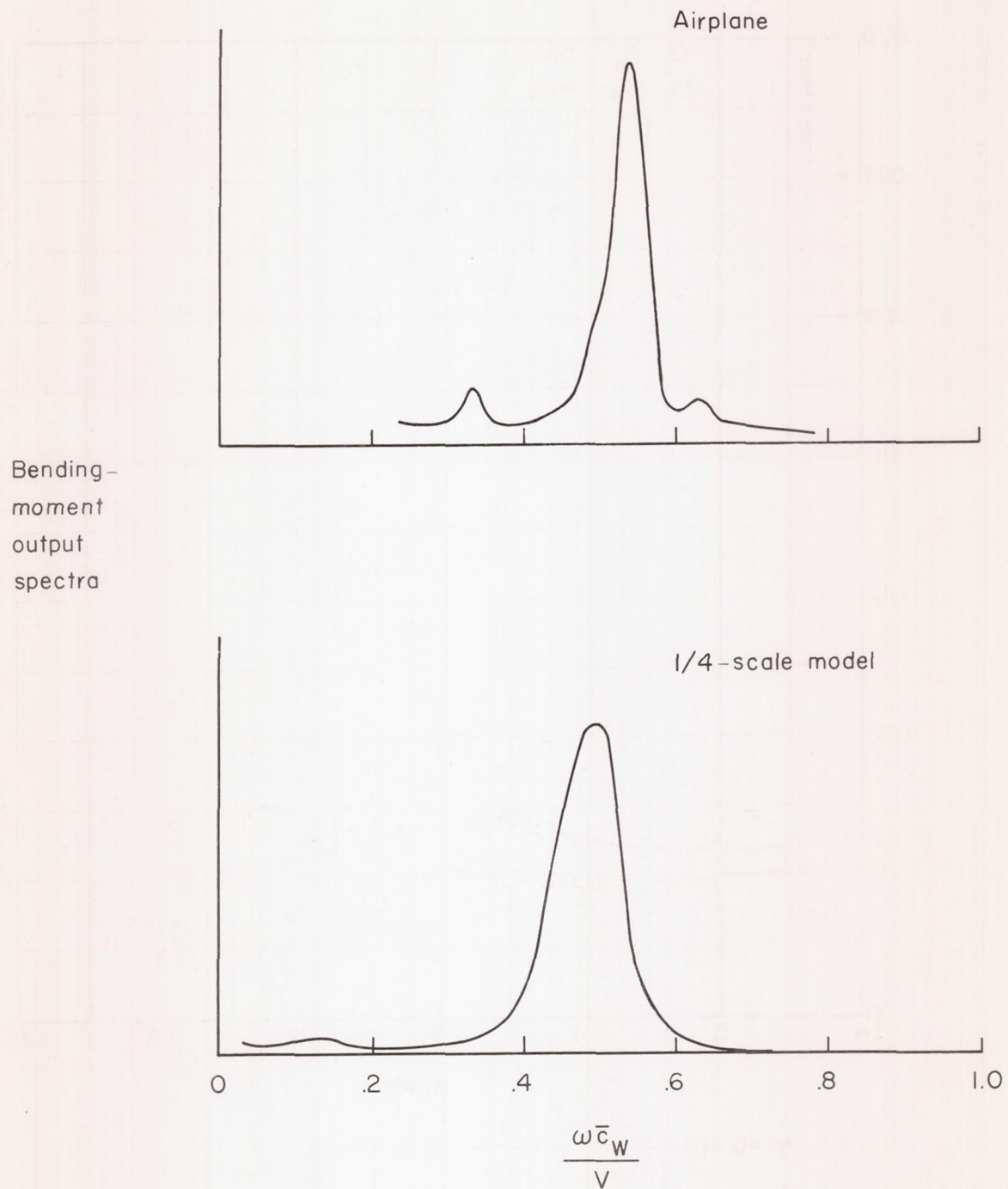


Figure 5.- Comparison of typical power spectra of wing bending moments during buffeting of airplane and 1/4-scale model.

CONFIDENTIAL

30

CONFIDENTIAL

NACA RM 158F25

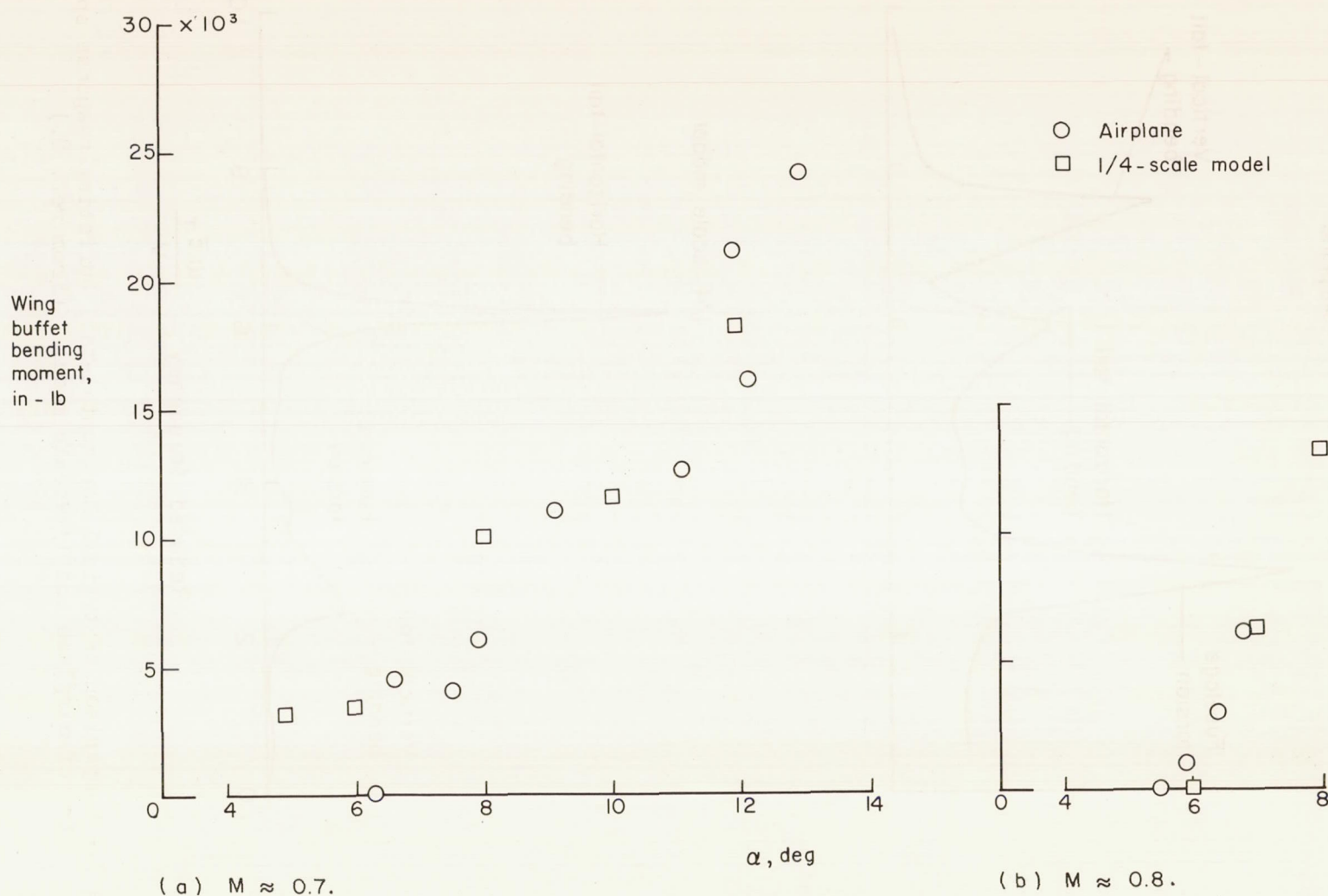


Figure 6.- Comparison of wing buffet bending moments measured in flight to bending moments extrapolated from 1/4-scale-model results.

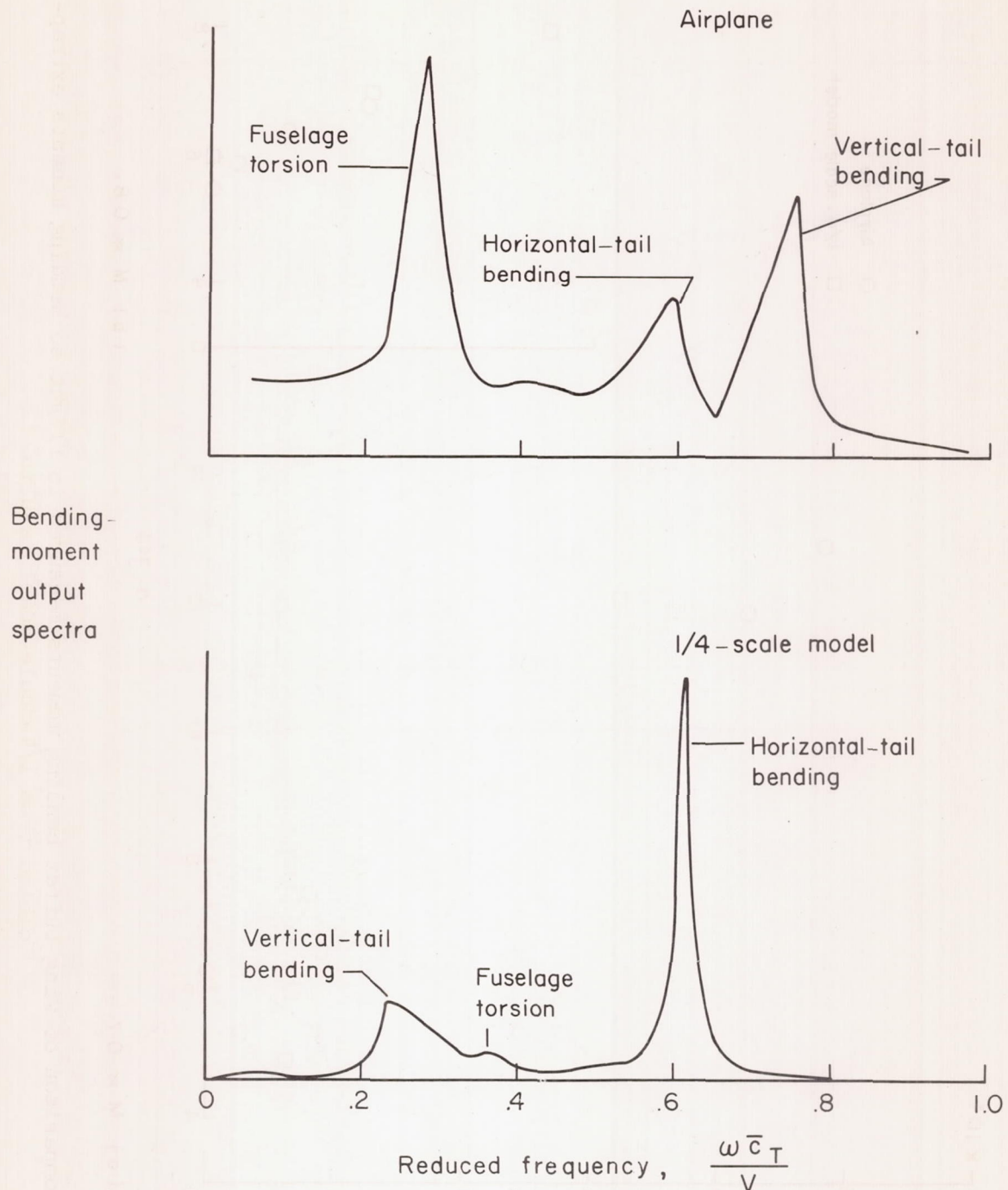


Figure 7.- Comparison of typical horizontal-tail buffeting response spectra of airplane and 1/4-scale model. (From ref. 8.)

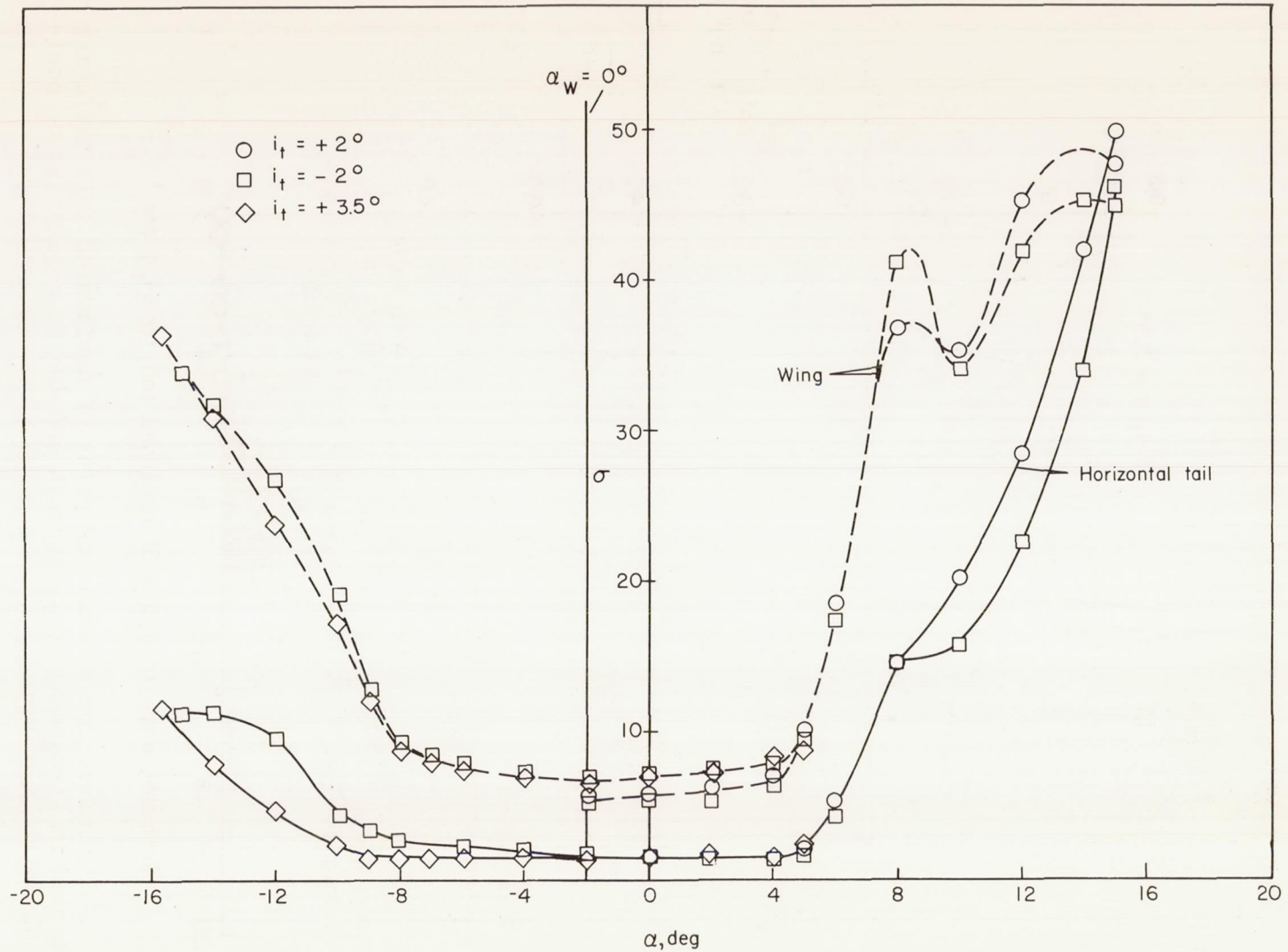


Figure 8.- Variation of rms bending moments with angle of attack for various values of horizontal-tail incidence angle.  $M = 0.40$ .

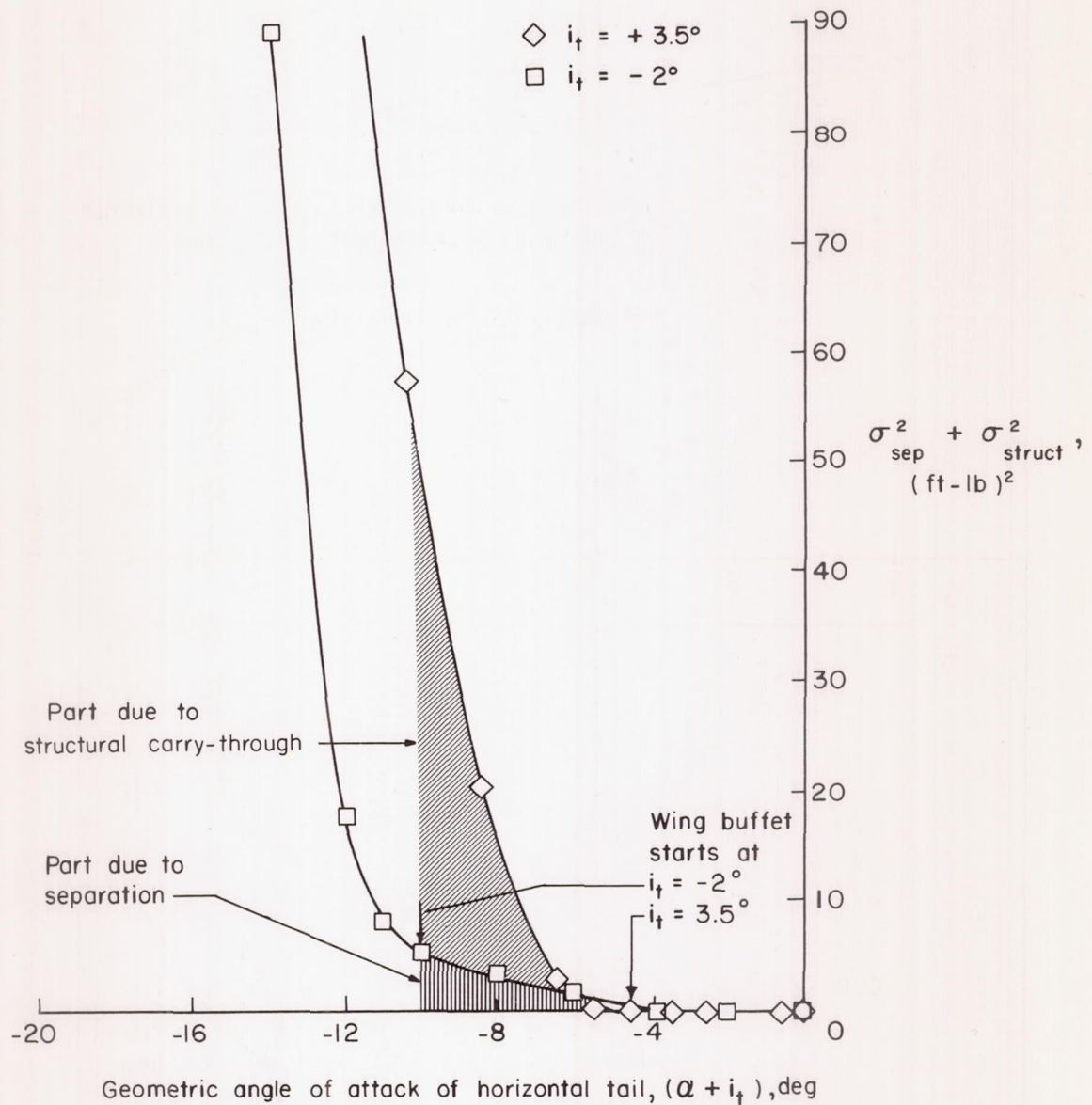
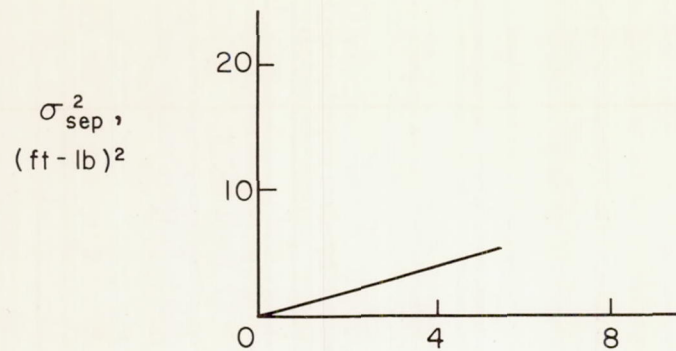
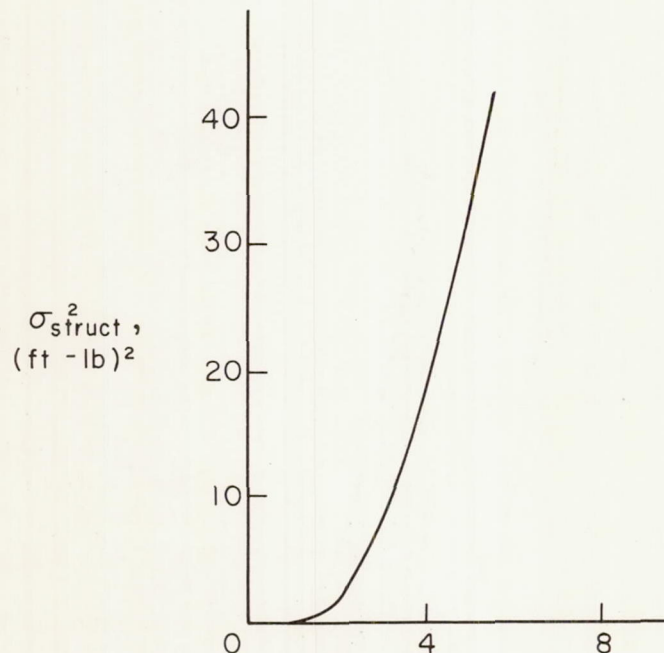


Figure 9.- Procedure for determining parts of horizontal tail buffeting loads due to structural carry-through and due to separation on horizontal tail.  $M = 0.40$ .



Increment in geometric angle of horizontal tail beyond separation point, deg

(a) Part due to separation.



Increment in geometric angle of horizontal tail beyond start of wing buffet, deg

(b) Part due to structural carry-through.

Figure 10.- Variation of buffeting loads on horizontal tail due to separation and due to structural carry-through with increment in geometric angle of horizontal tail.  $M = 0.40$ .

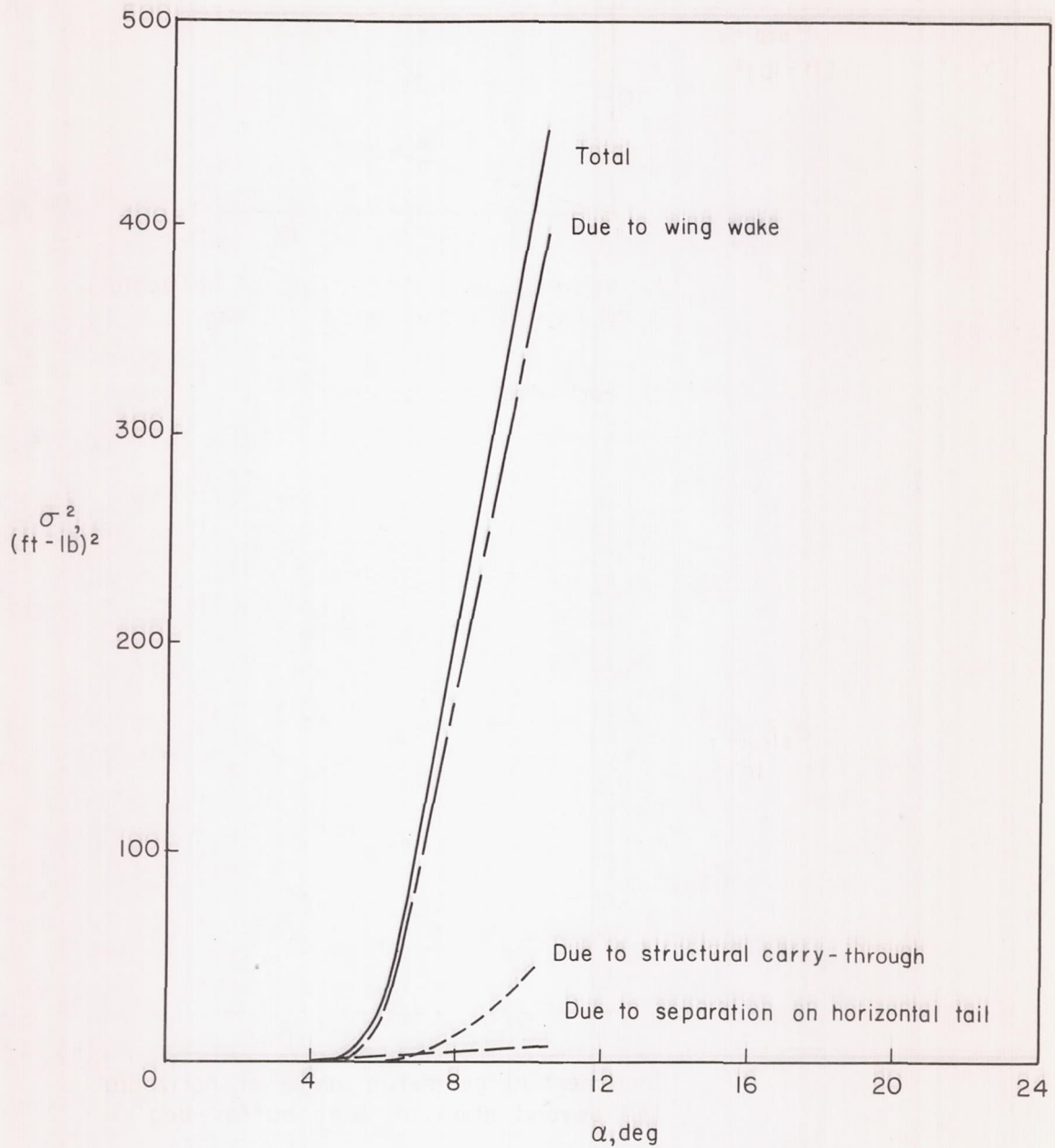


Figure 11.- Contribution of various sources of horizontal-tail buffeting loads.  $M = 0.40$ ;  $i_t = 2^\circ$ .





CONFIDENTIAL

CONFIDENTIAL